

Geometric representations of braid and Yang-Baxter gates

Kun Zhang,^{1,2,3} Kun Hao,^{3,4} Kwangmin Yu,⁵ Vladimir Korepin,⁶ and Wen-Li Yang^{2,3,4}

¹*School of Physics, Northwest University, Xi'an 710127, China*

²*Shaanxi Key Laboratory for Theoretical Physics Frontiers, Xi'an 710127, China*

³*Peng Huanwu Center for Fundamental Theory, Xi'an 710127, China*

⁴*Institute of Modern Physics, Northwest University, Xi'an 710127, China*

⁵*Computational Science Initiative, Brookhaven National Laboratory, Upton, New York 11973, USA*

⁶*C.N. Yang Institute for Theoretical Physics, Stony Brook University, New York 11794, USA*

(Dated: June 13, 2024)

Brick-wall circuits composed of the Yang-Baxter gates are integrable. It becomes an important tool to study the quantum many-body system out of equilibrium. To put the Yang-Baxter gate on the quantum computer, it has to be decomposed into the native gates of quantum computers. It is favorable to apply the least number of native two-qubit gates to construct the Yang-Baxter gate. We study the geometric representations of all X-type braid gates and their corresponding Yang-Baxter gates via the Yang-Baxterization. We find that the braid and Yang-Baxter gates can only exist on certain edges and faces of the two-qubit tetrahedron. We identify the parameters by which the braid and Yang-Baxter gates are the Clifford gate, the matchgate, and the dual-unitary gate. The geometric representations provide the optimal decompositions of the braid and Yang-Baxter gates in terms of other two-qubit gates. We also find that the entangling powers of the Yang-Baxter gates are determined by the spectral parameters. Our results provide the necessary conditions to construct the braid and Yang-Baxter gates on quantum computers.

I. INTRODUCTION

Quantum computers can efficiently solve problems that are unrealistic to be solved by classical computers [1]. Simulating many-body quantum systems is the major application of quantum computers in the current NISQ era [2]. The most popular model for quantum computation is the quantum circuit model. It is the quantum version of the classical reversible computation model. The quantum circuit model is composed of the initial state, unitary evolution realized by the single- and two-qubit gates, and the final state measurements. Arbitrary unitary evolution can be approximately constructed from the single- and two-qubit gates, known as the universal gate set [3, 4].

Although very few many-body systems can be exactly solved, these models lay the theoretical foundations for our understanding of the many-body system [5, 6]. One important category is called the Yang-Baxter integrable models, which are solved based on the Yang-Baxter equation [7–9]. The systematic method solving the Yang-Baxter integrable models is called the algebraic Bethe ansatz or the quantum inverse scattering method [10, 11]. See a recent review on the Yang-Baxter integrable models and their applications [12].

The essential ingredient to solve the Yang-Baxter integrable models is the R matrix, the solution of the Yang-Baxter equation. In the context of quantum computation, the unitary R matrix can work as the quantum gate, called the Yang-Baxter gate [13]. In the last twenty years, the interdisciplinary studies between the quantum integrable system and the quantum computation, especially based on the quantum circuit model, were developed in different directions, in either of which the Yang-Baxter gate plays the fundamental roles.

The unitary solution of parameter independent Yang-Baxter equation, also called the constant Yang-Baxter equation, gives the representation of braid group [14]. Here the Yang-Baxter gate is also called the braid gate. It can characterize the low-

dimensional topology but also can be viewed as the quantum gate generating the quantum entanglement [15, 16]. Therefore, the manipulation of quantum entanglement via the braid gate can be studied from the viewpoint of topology [17–20]. Then various quantum information protocols, such as quantum teleportation and entanglement swapping, can be understood from the viewpoint of topological entanglement [21–24].

In another research direction, the Yang-Baxter gate with the spectral parameter arises from the quantum simulation (based on the circuit model) of the integrable model. It is surprising that the simulation circuit obtained from decomposing the evolution operator into two-qubit gates, called the Trotterization, is still integrable [25–27]. The spectral parameter of the Yang-Baxter gate is interpreted as the Trotter step. Taking arbitrary values for the spectral parameter, the brick-wall circuit composed with the Yang-Baxter gates is always integrable [28]. The integrable circuit preserves many nice properties of the integrable model [29–34]. Furthermore, the integrable circuit may suggest a deep understanding of the quantum circuit model, where the evolution realized by the two-qubit gates is always factorized [35–37]. In experiments, the integrable circuit can not only benchmark the quantum computers but also provides the testbed to study the integrable-breaking dynamics [38–41].

Despite the vital importance of the Yang-Baxter gate, its completed characterizations are missing. For example, which two-qubit gates can be converted into the Yang-Baxter gates through the single-qubit gates? Which Yang-Baxter gates can be more easily realized on quantum computers (from the native two-qubit gates)? How to decompose the Yang-Baxter gate with the minimal applications of the native gates of quantum computers? We aim to answer the above questions by studying the geometric representation of braid and Yang-Baxter gates. Here the geometric representation refers to mapping the two-qubit gates on a three-dimensional tetrahe-

dron, where the two-qubit gates on the same point are locally equivalent (can be converted by the single-qubit gates) [42]. Then we give the optimal gate decompositions with respect to the number of CNOT gates of the braid and Yang-Baxter gates. In our study, we consider all the X-type braid gates and the Yang-Baxter gates obtained from braid gates through the Yang-Baxterization [43–45]. We clarify the conditions under which the braid and Yang-Baxter gates are the Clifford gates [46, 47], the matchgates [48, 49], and the dual unitary gates [50]. We calculate their entangling powers, which have been applied to the study of brick-wall circuits [51].

Our paper is organized as follows. In Sec. II, we review basic theories about the two-qubit gate, as well as its geometric representation. We present our results, namely the geometric representations of braid gate and Yang-Baxter gate in Secs. III and IV respectively. Sec. V is the conclusion. Appendix A gives the proof of Theorem 2. Appendix B shows the matrix expressions of the Yang-Baxter gates obtained from the Yang-Baxterization of the braid gates.

II. TETRAHEDRON OF TWO-QUBIT GATES

A. Nonlocal parameters and entangling power

Two-qubit gates U are elements of the $U(4)$ group. Since the global phase has no significance in quantum computation, we concentrate on the two-qubit gates belonging to the $SU(4)$ group. The nontrivial two-qubit gates are those that cannot be constructed from the single-qubit gates, namely $U \in SU(4) \setminus SU(2) \otimes SU(2)$. Then one can apply the Cartan decomposition to $U \in SU(4) \setminus SU(2) \otimes SU(2)$, which gives [52]

$$U = (V_1 \otimes V_2) U_{\text{core}}(\vec{a})(V_3 \otimes V_4), \quad (1)$$

with the core of the two-qubit gate

$$U_{\text{core}}(\vec{a}) = \exp\left(\frac{i}{2}(a_1(\sigma_x \otimes \sigma_x) + a_2(\sigma_y \otimes \sigma_y) + a_3(\sigma_z \otimes \sigma_z))\right). \quad (2)$$

Here $V_k \in SU(2)$ ($k = 1, 2, 3, 4$) are the single-qubit gates and $\sigma_{x,y,z}$ are Pauli matrices. Therefore, only $\vec{a} = (a_1, a_2, a_3)$, called the nonlocal parameters, characterizes the intrinsic properties of two-qubit gates. For simplicity, we use

$$[U] = [a_1, a_2, a_3], \quad (3)$$

to denote the nonlocal parameters of U . We say that two-qubit gates are locally equivalent if these two-qubit gates have the same nonlocal parameters. In other words, two-qubit gates with the same nonlocal parameters only differ by some single-qubit gates.

Quantities associated with the two-qubit gate, which are invariant under the action of single-qubit gates, are called local invariants. It is expected that the local invariants are

given by $[a_1, a_2, a_3]$. It has been shown that the complete set of local invariants of the two-qubit gate is given by the spectrum of $L = Q^T \Lambda Q$ [53], which has the eigenvalues $\Lambda = \{e^{i(-a_1+a_2+a_3)}, e^{i(a_1-a_2+a_3)}, e^{i(a_1+a_2-a_3)}, e^{-i(a_1+a_2+a_3)}\}$. Specifically, the characteristic polynomial of L is completely determined by $\text{Tr}(\Lambda)$ and $\text{Tr}(\Lambda^2)$. Therefore, the local invariants are functions of $\text{Tr}(\Lambda)$ and $\text{Tr}(\Lambda^2)$.

Two-qubit gates with different nonlocal parameters may have different abilities to generate the entanglement. For example, the CNOT gate given by

$$\text{CNOT} = |0\rangle\langle 0| \otimes \mathbb{1}_2 + |1\rangle\langle 1| \otimes \sigma_x, \quad (4)$$

has the nonlocal parameters $[\text{CNOT}] = [\pi/2, 0, 0]$, which can generate Bell states from the product states (with the help of single-qubit gates). However, the SWAP gate defined by

$$\text{SWAP} = \frac{1}{2}(\mathbb{1}_2 + \sigma_x \otimes \sigma_x + \sigma_y \otimes \sigma_y + \sigma_z \otimes \sigma_z) \quad (5)$$

has $[\text{SWAP}] = [\pi/2, \pi/2, \pi/2]$, which only permutes between two qubits, and can not create any entanglement from the product states. For the XY interaction qubit, it is natural to give the iSWAP gate [54]

$$\text{iSWAP} = \frac{1}{2}(\mathbb{1}_2 + i\sigma_x \otimes \sigma_x + i\sigma_y \otimes \sigma_y + \sigma_z \otimes \sigma_z), \quad (6)$$

which has $[\text{iSWAP}] = [\pi/2, \pi/2, 0]$. Therefore, it can generate entangled states from the product states.

To quantify the entanglement-generation ability of two-qubit gates, consider [55]

$$e_p(U) = \overline{E(U|\psi_1\rangle \otimes |\psi_2\rangle)}_{|\psi_1\rangle \otimes |\psi_2\rangle}, \quad (7)$$

with the linear entropy

$$E(|\Psi\rangle) = 1 - \text{Tr}_1 \rho^2, \quad (8)$$

and $\rho = \text{Tr}_2 |\Psi\rangle\langle\Psi|$. The overline means taking the average over all product states $|\psi_1\rangle \otimes |\psi_2\rangle$ with the uniform distribution. We call $e_p(U)$ as the entangling power of two-qubit gates. Because of the simple decomposition given in Eq. (1), one can find that the entangling power of the two-qubit gate is [56]

$$e_p(U) = \frac{2}{9} \left(1 - \frac{1}{16} |\text{Tr}(\Lambda)|^2\right), \quad (9)$$

with the local invariants of the two-qubit gate

$$\begin{aligned} |\text{Tr}(\Lambda)|^2 &= 16 (\cos^2 a_1 \cos^2 a_2 \cos^2 a_3 + \sin^2 a_1 \sin^2 a_2 \sin^2 a_3). \end{aligned} \quad (10)$$

We can see that $0 \leq e_p(U) \leq 2/9$. The CNOT gate with the nonlocal parameter $[\text{CNOT}] = [\pi/2, 0, 0]$ has the maximal entangling power $e_p(\text{CNOT}) = 2/9$. The SWAP gate with $[\text{SWAP}] = [\pi/2, \pi/2, \pi/2]$ has zero entangling power. Any two-qubit gate with nonzero entangling power can form a universal gate set with the single-qubit gates [57, 58].

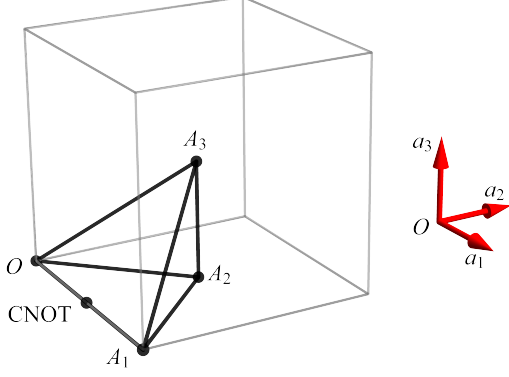


FIG. 1. Geometric representation of the two-qubit gate $U = [a_1, a_2, a_3]$. The tetrahedron $OA_1A_2A_3$ has the vertices $O = [0, 0, 0]$, $A_1 = [\pi, 0, 0]$, $A_2 = [\pi/2, \pi/2, 0]$, and $A_3 = [\pi/2, \pi/2, \pi/2]$.

Naturally, based on the value of the nonlocal parameters $[a_1, a_2, a_3]$, we can map each two-qubit gate on a point in the three-dimensional space, namely the 3-Torus (because of the periodicity of $[a_1, a_2, a_3]$). Even if we only consider the cube with length π , different points inside the cube may correspond to the two-qubit gates which are locally equivalent. For example, the two-qubit gate with $[\theta, 0, 0]$ is locally equivalent to the two-qubit gate with $[0, 0, \theta]$ by applying the Hadamard transformation.

One can apply the Weyl group to remove such ambiguity, called the Weyl chamber [42]. Then the cube can be divided into 24 Weyl chambers. Each chamber is a tetrahedron. Choose the tetrahedron with the vertices $O = [0, 0, 0]$, $A_1 = [\pi, 0, 0]$, $A_2 = [\pi/2, \pi/2, 0]$, and $A_3 = [\pi/2, \pi/2, \pi/2]$, namely the region with $\pi - a_2 \geq a_1 \geq a_2 \geq a_3 \geq 0$. See Fig. 1. Different points in one Weyl chamber correspond to the different nonlocal two-qubit gates (except the points on the

OA_1A_2 base). The middle of OA_1 represents the CNOT gate with $[\text{CNOT}] = [\pi/2, 0, 0]$. The SWAP gate is at the point A_3 with $[\text{SWAP}] = [\pi/2, \pi/2, \pi/2]$. Except for the vertices O , A_1 , and A_3 , all two-qubit gates have nonzero entangling powers. Note that the two-qubit gates that have the same entangling powers may be not locally equivalent.

B. Decomposition of two-qubit gate

Quantum computers are equipped with several native gates. Then arbitrary unitary operation can be constructed or approximately constructed from those gates [1]. How to construct arbitrary two-qubit gate is well studied [59–63]. The Cartan decomposition of two-qubit gate in Eq. (1) naturally gives the following decomposition criterion [59].

Theorem 1. Any two-qubit gate $[U] = [a_1, a_2, a_3]$ can be constructed from minimal n ($n \geq 3$) applications of $U'(\theta)$ with $[U(\theta)'] = [\theta, 0, 0]$, if the nonlocal parameters satisfy $0 \leq a_1 + a_2 + a_3 \leq n\theta$ or $a_1 - a_2 - a_3 \geq \pi - n\theta$.

Therefore any two-qubit gate can be constructed from at most three CNOTs. Two-qubit gates belong to $SO(4)$ have the nonlocal parameters $a_3 = 0$. Consequently, their decompositions only need at most two CNOTs [60, 61].

Applying the trick $\text{CNOT}(\mathbb{1}_2 \otimes \sigma_z)\text{CNOT} = \sigma_z \otimes \sigma_z$, then we have

$$e^{-\frac{i}{2}\theta(\sigma_z \otimes \sigma_z)} = \begin{array}{c} \bullet \quad \bullet \\ | \quad | \\ \oplus \quad \oplus \\ \boxed{R_z(\theta)} \\ \oplus \quad \oplus \end{array} \quad (11)$$

with the single-qubit rotation gate $R_z(\theta) = e^{-\frac{i}{2}\theta\sigma_z}$. Therefore any two-qubit gate can be decomposed with six CNOTs. After some simplifications, we have the optimal CNOT decomposition for any two-qubit gate (given by the universal gate set $\{R_z(\theta), H, \text{CNOT}\}$) [64]

$$U = \begin{array}{c} \boxed{V_3} \quad \bullet \quad \boxed{H} \quad \boxed{S} \quad \boxed{R_z^\dagger(a_2)} \\ | \quad | \quad | \quad | \quad | \\ \oplus \quad \oplus \quad \oplus \quad \oplus \quad \oplus \\ \boxed{V_4} \quad \oplus \quad \boxed{R_z^\dagger(a_1)} \quad \oplus \quad \boxed{R_z(a_3)} \quad \boxed{H} \quad \oplus \quad \boxed{S^\dagger} \quad \boxed{H} \quad \boxed{V_1} \\ | \quad | \quad | \quad | \quad | \\ \oplus \quad \oplus \quad \oplus \quad \oplus \quad \oplus \\ \boxed{V_4} \quad \oplus \quad \boxed{R_z^\dagger(a_1)} \quad \oplus \quad \boxed{R_z(a_3)} \quad \boxed{H} \quad \oplus \quad \boxed{S} \quad \boxed{H} \quad \boxed{V_2} \end{array} \quad (12)$$

with the Hadamard gate $H = (\sigma_x + \sigma_z)/\sqrt{2}$ and the phase gate $S = \text{diag}\{1, i\}$. Note that we have $S \cong R_z(\pi/2)$. The symbol \cong represents the equivalent relation up to the global phase difference. The nonlocal parameters are interchangeable because of the commutative of $\sigma_x \otimes \sigma_x$, $\sigma_y \otimes \sigma_y$, and $\sigma_z \otimes \sigma_z$. Note that the above decomposition is not optimal if $a_3 = 0$, since only two CNOTs are required.

III. GEOMETRIC REPRESENTATIONS AND DECOMPOSITIONS OF BRAID GATES

A. Two-qubit braid gates

The braid group relation or the constant Yang-Baxter equation characterizes the low-dimensional topology [14]. The topological entanglement can be described by the corresponding knot invariants. Then one can consider the unitary rep-

representation of the braid group. It works as a two-qubit gate, which can generate quantum entanglement. In the qubit representation, how to construct the braid matrix or the unitary braid gate is well studied [65–67].

The braid group has the generator b_j with $j = 1, 2, \dots, n-1$ satisfying

$$b_j b_{j\pm 1} b_j = b_{j\pm 1} b_j b_{j\pm 1}, \quad (13a)$$

$$b_j b_k = b_k b_j, \quad |j - k| \geq 2. \quad (13b)$$

In the context of quantum computation, we consider the braid group representation given by $b_j = \mathbb{1}_2 \otimes \mathbb{1}_2 \otimes \dots \otimes B_{j,j+1} \otimes \dots \otimes \mathbb{1}_2 \otimes \mathbb{1}_2$, where $B_{j,j+1}$ is a two-qubit gate acting on the qubits j and $j+1$. Here B is called the braid gate. We omit the subscripts in the following for simplicity. Note that the commutative relation of b_j is satisfied automatically. The braid relation becomes

$$(B \otimes \mathbb{1}_2)(\mathbb{1}_2 \otimes B)(B \otimes \mathbb{1}_2) = (\mathbb{1}_2 \otimes B)(B \otimes \mathbb{1}_2)(\mathbb{1}_2 \otimes B). \quad (14)$$

Therefore, any two-qubit gate that satisfies the above relation is a braid gate.

All solutions of B in the two-qubit cases are known [65, 66]. Note that one has to add the unitary condition (to be a valid quantum gate). The core of the two-qubit gate U_{core} defined in Eq. (2) is the X-type two-qubit gate. There are in total four X-type braid gates [68]. At the two-qubit basis $\{|00\rangle, |01\rangle, |10\rangle, |11\rangle\}$, the four braid gates have the forms

$$B_I = \begin{pmatrix} e^{i\varphi_1} & 0 & 0 & 0 \\ 0 & 0 & e^{i\varphi_2} & 0 \\ 0 & e^{i\varphi_3} & 0 & 0 \\ 0 & 0 & 0 & e^{i\varphi_4} \end{pmatrix}, \quad (15a)$$

$$B_{II} = \begin{pmatrix} 0 & 0 & 0 & e^{i\varphi_2} \\ 0 & e^{i\varphi_1} & 0 & 0 \\ 0 & 0 & e^{i\varphi_1} & 0 \\ e^{i\varphi_3} & 0 & 0 & 0 \end{pmatrix}, \quad (15b)$$

$$B_{III} = \begin{pmatrix} \cos \varphi_1 & 0 & 0 & \sin \varphi_1 e^{i\varphi_2} \\ 0 & -i \sin \varphi_1 & -\cos \varphi_1 & 0 \\ 0 & -\cos \varphi_1 & -i \sin \varphi_1 & 0 \\ -\sin \varphi_1 e^{-i\varphi_2} & 0 & 0 & \cos \varphi_1 \end{pmatrix}, \quad (15c)$$

$$B_{IV} = \frac{1}{\sqrt{2}} \begin{pmatrix} 1 & 0 & 0 & e^{i\varphi_1} \\ 0 & 1 & 1 & 0 \\ 0 & -1 & 1 & 0 \\ -e^{-i\varphi_1} & 0 & 0 & 1 \end{pmatrix}. \quad (15d)$$

The parameters can be taken arbitrarily $\varphi_j \in [0, 2\pi)$. In the following, we always take φ_j as the braid gate parameters.

B. Geometric representations and decompositions

Consider the universal gate set $\{R_z(\theta), H, \text{CNOT}\}$. Based on the standard decomposition of the two-qubit gate given in Eq. (1), we have the decompositions of braid gates shown in Fig. 2. The parameters ϕ_I of braid gate B_I are defined as

$$\phi_{I,1} = \frac{1}{2}(-\varphi_1 - \varphi_2 + \varphi_3 + \varphi_4), \quad (16a)$$

$$\phi_{I,2} = \frac{1}{2}(-\varphi_1 + \varphi_2 - \varphi_3 + \varphi_4), \quad (16b)$$

$$\phi_{I,3} = \frac{1}{2}(-\varphi_1 + \varphi_2 + \varphi_3 - \varphi_4). \quad (16c)$$

The braid gate B_{II} has the defined parameters

$$\phi_{II,1} = \frac{1}{2}(-\varphi_2 + \varphi_3), \quad (17a)$$

$$\phi_{II,2} = \frac{1}{2}(-\varphi_2 + 2\varphi_1 - \varphi_3). \quad (17b)$$

Note that both $B_I \text{SWAP}$ and $B_{II} \text{SWAP}(\sigma_x \otimes \sigma_x)$ are diagonal matrices.

The braid gates have the nonlocal parameters

$$[B_I] = \frac{1}{2}[\pi, \pi, \pi - 2\phi_{I,3}], \quad (18a)$$

$$[B_{II}] = \frac{1}{2}[\pi, \pi, \pi - 2\phi_{II,2}], \quad (18b)$$

$$[B_{III}] = \frac{1}{2}[\pi, \pi, \pi - 4\varphi_1], \quad (18c)$$

$$[B_{IV}] = \frac{1}{2}[\pi, 0, 0]. \quad (18d)$$

We can see that the braid gates $B_{I,II,III}$ are all on the edge A_2A_3 of the two-qubit tetrahedron. See Fig. 3. When $B_{I,II,III}$ are not at the point A_2 , namely without any vanishing nonlocal parameters, their constructions require minimal three CNOTs, therefore the decompositions in Fig. 2 are optimal. The braid gate B_{IV} is locally equivalent to the CNOT.

It is straightforward to calculate the entangling powers of the four braid gates. Specifically, we have

$$e_p(B_I) = \frac{2}{9} \sin^2 \phi_{I,3}, \quad (19a)$$

$$e_p(B_{II}) = \frac{2}{9} \sin^2 \phi_{II,2}, \quad (19b)$$

$$e_p(B_{III}) = \frac{2}{9} \sin^2 (2\varphi_1), \quad (19c)$$

$$e_p(B_{IV}) = \frac{2}{9}. \quad (19d)$$

When Braid gates $B_{I,II,III}$ (with $\phi_{I,3} = 0$, or $\phi_{II,2} = 0$, or $\varphi_1 = 0$) are locally equivalent to the SWAP gate, they have zero entangling power.

Clifford gates are elements of the Clifford group, which preserves the Pauli group, therefore circuits only composed with Clifford gates can be classically simulated [46, 47]. Another equivalent definition of the Clifford gate is the quantum gate can be decomposed with $\{H, S, \text{CNOT}\}$. Based

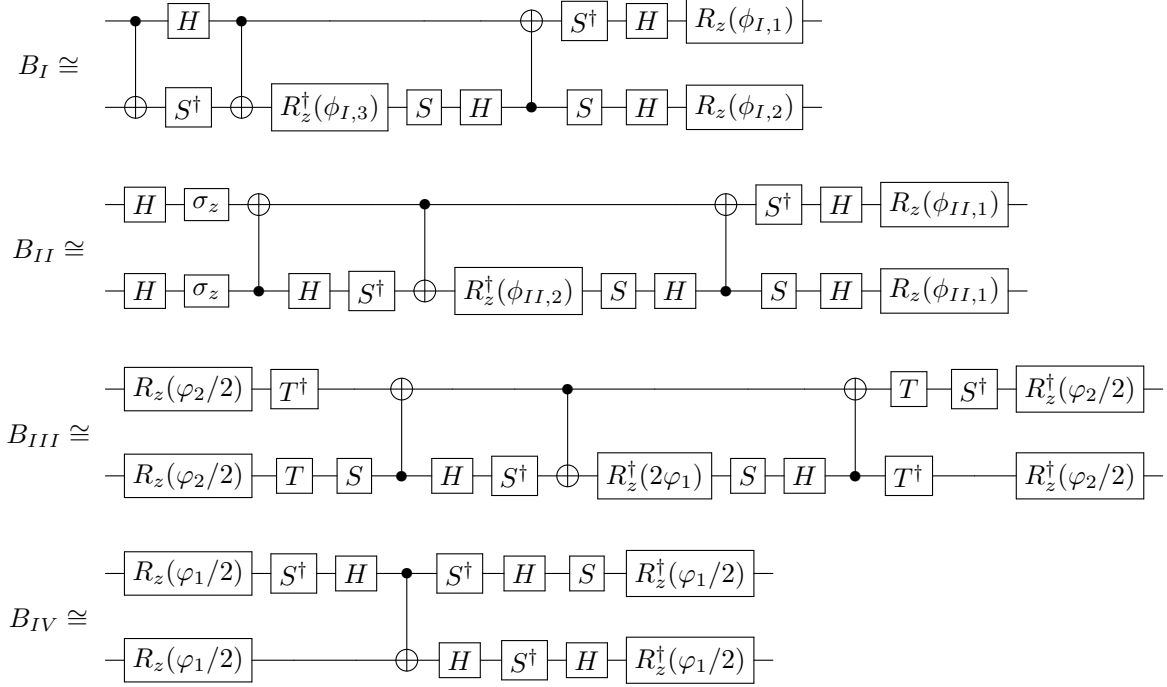


FIG. 2. Decomposition of braid gates B_I (15a), B_{II} (15b), B_{III} (15c), and B_{IV} (15d) into the universal gate set $\{R_z(\theta), H, \text{CNOT}\}$. The symbol \cong means a global phase difference. The angles ϕ_I are defined in Eq. (16a)-(16c). The angles ϕ_{II} are defined in Eq. (17a)-(17b). Here S is the phase gate with $S \cong R_z(\pi/2)$, and T is the $\pi/8$ gate with $T \cong R_z(\pi/4)$.

| | Clifford gate | Matchgate | Dual unitary gate |
|-----------|---|-----------------------|-------------------|
| B_I | $\phi_{I,1}, \phi_{I,2}, \phi_{I,3} \in \{k\pi/2, k \in \mathbb{Z}\}$ | $\phi_{I,3} = \pi/2$ | Always |
| B_{II} | $\phi_{II,1}, \phi_{II,2} \in \{k\pi/2, k \in \mathbb{Z}\}$ | $\phi_{II,2} = \pi/2$ | Always |
| B_{III} | $\varphi_1 \in \{k\pi/4, k \in \mathbb{Z}\}$ and $\varphi_2 \in \{k\pi + \pi/2, k \in \mathbb{Z}\}$ | Cannot | Always |
| B_{IV} | $\varphi_1 \in \{k\pi, k \in \mathbb{Z}\}$ | Always | Cannot |

TABLE I. Conditions for braid gates B_I (15a), B_{II} (15b), B_{III} (15c), and B_{IV} (15d) to be the Clifford, the matchgate, and the dual unitary gate.

on the gate decomposition of the four braid gates, we know that the braid gate B_I is a Clifford gate if $\phi_{I,1}, \phi_{I,2}, \phi_{I,3} \in \{k\pi/2, k \in \mathbb{Z}\}$; the braid gate B_{II} is a Clifford gate if $\phi_{II,1}, \phi_{II,2} \in \{k\pi/2, k \in \mathbb{Z}\}$; the braid gate B_{III} is a Clifford gate if $\varphi_1 \in \{k\pi/4, k \in \mathbb{Z}\}$ and $\varphi_2 \in \{k\pi + \pi/2, k \in \mathbb{Z}\}$; the braid gate B_{IV} is a Clifford gate if $\varphi_1 \in \{k\pi, k \in \mathbb{Z}\}$. We summary the results in Table I.

Matchgate is a special family of X-type two-qubit gates. Quantum circuits only composed with the matchgates acting on the nearest neighbor qubits is another family of circuits that is classically tractable [48, 49]. Matchgate circuit can be mapped to the dynamics of the free fermion model [69]. The necessary condition of being a matchgate is to have a vanishing nonlocal parameter [70]. We can check that the braid gate B_I is a matchgate if $\phi_{I,3} = \pi/2$; the braid gate B_{II} is a matchgate if $\phi_{II,2} = \pi/2$; the braid gate B_{III} can not be a matchgate; the braid gate B_{IV} is always a matchgate.

It is interesting to see that two-qubit gates on the edge A_2A_3 belong to the dual-unitary gates, which are still unitary if the

space and time indexes are exchanged [50]. The dynamical correlation functions of the brick-wall circuit composed with the dual-unitary gate can be exactly calculated. From Fig. 3, we see that braid gates B_I , B_{II} , and B_{IV} are all dual-unitary, while B_{III} is not.

IV. GEOMETRIC REPRESENTATIONS AND DECOMPOSITIONS OF YANG-BAXTER GATES

A. Yang-Baxterization

In the braid relation (14), the braid parameters are all the same. The braid relation can be generalized to a parameter-

B. Yang-Baxter gates from Yang-Baxterization

The braid gate B_I has the eigenvalues

$$\lambda_{I,1} = -e^{\frac{i}{2}(\varphi_2 + \varphi_3)}, \quad (28a)$$

$$\lambda_{I,2} = e^{i\varphi_1}, \quad (28b)$$

$$\lambda_{I,3} = e^{\frac{i}{2}(\varphi_2 + \varphi_3)}, \quad (28c)$$

$$\lambda_{I,4} = e^{i\varphi_4}. \quad (28d)$$

If we consider the Yang-Baxterization with four distinct eigenvalues, it does not give the correct R matrix. Therefore we restrict to $\varphi_1 = \varphi_4$, namely three distinct eigenvalues. The braid gate B_I with $\varphi_1 = \varphi_4$ has a simple relation with B_{II} given by

$$B_I(\varphi_1 = \varphi_4) = (\mathbb{1}_2 \otimes \sigma_x) B_{II} (\mathbb{1}_2 \otimes \sigma_x). \quad (29)$$

It suggests that they have the same eigenvalues, denoted as

$$\lambda_{II,1} = -e^{\frac{i}{2}(\varphi_2 + \varphi_3)}, \quad (30a)$$

$$\lambda_{II,2} = e^{i\varphi_1}, \quad (30b)$$

$$\lambda_{II,3} = e^{\frac{i}{2}(\varphi_2 + \varphi_3)}. \quad (30c)$$

Note that the $R(x)$ matrices obtained from Eq. (26) preserves the transformation, since Pauli matrix σ_x is Hermitian.

Consider the braid gate B_{III} , which has the eigenvalues

$$\lambda_{III,1} = -e^{i\varphi_1}, \quad (31a)$$

$$\lambda_{III,2} = e^{-i\varphi_1}, \quad (31b)$$

$$\lambda_{III,3} = e^{i\varphi_1}. \quad (31c)$$

The eigenvalues are only dependent on the braid parameter φ_1 .

The Yang-Baxterization of three distinct eigenvalues, namely Eq. (26) gives the following R matrices

$$R_{l,1}(x) = \alpha(x, \lambda_{l,3}) B_l + \beta(x, \lambda_{l,1}, \lambda_{l,2}, \lambda_{l,3}) \mathbb{1} + \gamma(x, \lambda_{l,1}) B_l^\dagger, \quad (32)$$

with $l \in \{I, II, III\}$. We call them the first kind of R matrix (or Yang-Baxter gate) of B_l . For B_{III} , it admits a representation of BMW algebra, therefore the solution of the Yang-Baxter equation is guaranteed. Although the braid gates B_I and B_{II} do not have the BMW algebra representation, they satisfy the necessary condition for Yang-Baxterization given in [45], therefore $R_{II,1}$ and $R_{II,2}$ also satisfy the Yang-Baxter equation.

We observe that the eigenvalues of B_I , B_{II} , and B_{III} both satisfy

$$\beta(x, \lambda_{l,2}, \lambda_{l,1}, \lambda_{l,3}) = 0, \quad (33a)$$

$$\beta(x, \lambda_{l,1}, \lambda_{l,3}, \lambda_{l,2}) = 0, \quad (33b)$$

with $l \in \{I, II, III\}$. Here β is the coefficient of the Yang-Baxterization in Eq. (26). Therefore, the three-eigenvalue Yang-Baxterization reduces to the two-eigenvalue

Yang-Baxterization. Specifically, we have another two types of R matrices

$$R_{l,2}(x) = \alpha(x, \lambda_{l,3}) B_l + \gamma(x, \lambda_{l,2}) B_l^\dagger, \quad (34a)$$

$$R_{l,3}(x) = \alpha(x, \lambda_{l,2}) B_l + \gamma(x, \lambda_{l,1}) B_l^\dagger, \quad (34b)$$

with $l \in \{I, II, III\}$. We call them the second and third kinds of R matrices (or Yang-Baxter gate) of B_l . Note that the second and third kinds of Yang-Baxter gates are obtained from the eigenvalue permutation $\lambda_1 \leftrightarrow \lambda_2$ and $\lambda_2 \leftrightarrow \lambda_3$ of the first kind. The unitary condition requires that the spectral parameter in the first kind $R_{l,1}$ is real. From Theorem 2, we know that $R_{l,2}$ and $R_{l,3}$ are unitary if the spectral parameter x is also real, therefore work as two-qubit gates.

Specifically, $R_{I,1}$ is the R matrix of the XXZ model [77]. The braid gate parameter in $R_{I,1}$ corresponds to the anisotropic coupling of the spin chain. The $R_{III,1}$ matrix can also be obtained from the trigonometric limits of elliptic R matrix [78]. Moreover, the $R_{III,1}$ matrix is locally equivalent to the R matrix of the sine-Gordon model [79]. The matrix expressions of $R_{l,1}$, $R_{l,2}$, and $R_{l,3}$, namely total nine R gates, can be found in Appendix B.

The braid gate B_{IV} only has two distinct eigenvalues, $\lambda_{IV,1} = e^{i\pi/4}$ and $\lambda_{IV,2} = e^{-i\pi/4}$, therefore the Yang-Baxterization gives a unique R matrix, namely

$$R_{IV}(\chi) \cong \begin{pmatrix} \cos \chi & 0 & 0 & e^{i\varphi_1} \sin \chi \\ 0 & \cos \chi & \sin \chi & 0 \\ 0 & -\sin \chi & \cos \chi & 0 \\ -e^{-i\varphi_1} \sin \chi & 0 & 0 & \cos \chi \end{pmatrix}, \quad (35)$$

with the real spectral parameter \dagger

$$x = \tan(\chi - \pi/4). \quad (36)$$

The optimal gate and pulse constructions of $R_{IV}(\chi)$ with $\varphi_1 = 0$ have been detailed studied in [64].

C. Geometric representations of Yang-Baxter gates

Through some analysis, we find the nonlocal parameters of $R_{I,1}$ are

$$[R_{I,1}] = [a_{I,1}, a_{I,1}, c_{I,1}], \quad (37)$$

with

$$a_{I,1} = \arccos \left(\sqrt{\frac{1 - \cos 2\varphi}{\cosh 2\mu - \cos 2\varphi}} \right), \quad (38a)$$

$$c_{I,1} = \frac{i}{2} \ln \left(\frac{\sin(\varphi + i\mu)}{\sin(\varphi - i\mu)} \right). \quad (38b)$$

\dagger It is a non-conventional way to parameterize the spectral parameter. Therefore we denote it as χ , to distinguish it from μ .

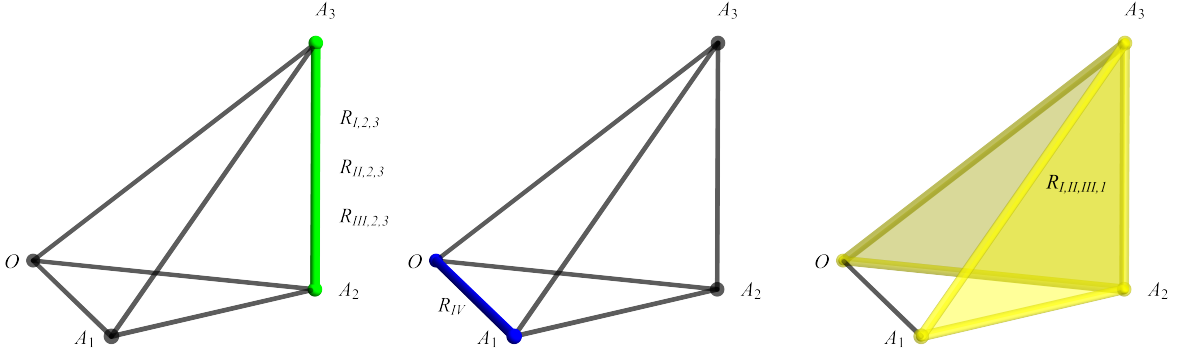


FIG. 4. Geometric representations of Yang-Baxter gates obtained from braid gates. Yang-Baxter gates $R_{I,1}$, $R_{I,2}$, and $R_{I,3}$ with $l \in \{I, II, III\}$ are defined in Eqs. (32), (34a), and (34b) respectively. The Yang-Baxter gate R_{IV} is given in Eq. (35).

Here $\mu = \ln x$ with $x > 0$ and $\varphi = (\varphi_2 + \varphi_3)/2 - \varphi_1$. Therefore, the nonlocal parameters are jointly determined by the spectral parameter μ and the braid gate parameter φ . The Yang-Baxter gates obtained from B_I are locally equivalent to the ones obtained from B_{II} , suggested by Eq. (29). Therefore, we have

$$[R_{II,1}] = [R_{I,1}]. \quad (39)$$

Note that $a_{I,1} \in [0, \pi/2]$ and $c_{I,1} \in [-\pi/2, \pi/2]$. When $\mu \rightarrow -\infty$, we restore the braid gate B_I , corresponding to the boundary condition $R(x \rightarrow 0) \rightarrow B$.

The two-qubit tetrahedron requires the range $\pi - a_{I,1} \geq a_{I,1} \geq c_{I,1} \geq 0$. We can always gauge the nonlocal parameters in the two-qubit tetrahedron through the local transformations. For example, if $c_{I,1} < 0$, we have the two-qubit tetrahedron $[\pi - a_{I,1}, a_{I,1}, -c_{I,1}]$. See Fig. 4. We can see that $R_{I,1}$ and $R_{I,2}$ are on the faces OA_1A_2 and OA_2A_3 .

The Yang-Baxter gates $R_{I,2}$ and $R_{I,3}$ are SWAP-like gates (exchanging states $|01\rangle$ and $|10\rangle$ with some phases). See the Appendix B. Therefore, they have similar geometric representations as B_I . Specifically, they have the nonlocal parameters

$$[R_{I,2}] = \left[\frac{\pi}{2}, \frac{\pi}{2}, \frac{\pi}{2} - \varphi_{I,2} \right], \quad (40a)$$

$$[R_{I,3}] = \left[\frac{\pi}{2}, \frac{\pi}{2}, \frac{\pi}{2} - \varphi_{I,3} \right], \quad (40b)$$

with

$$\varphi_{I,2} = \frac{1}{i} \ln \left(\frac{\sin(\frac{1}{2}(\varphi - i\mu))}{\sin(\frac{1}{2}(\varphi + i\mu))} \right), \quad (41a)$$

$$\varphi_{I,3} = \frac{1}{i} \ln \left(\frac{\cos(\frac{1}{2}(\varphi + i\mu))}{\cos(\frac{1}{2}(\varphi - i\mu))} \right). \quad (41b)$$

Since the two nonlocal parameters of $R_{I,2}$ and $R_{I,3}$ are constant, we can always gauge the third in the range $[0, \pi/2]$. Therefore, $R_{I,2}$ and $R_{I,3}$ are on the edge A_2A_3 of the two-qubit tetrahedron. Moreover, because of Eq. (29), we have

$$[R_{II,2}] = [R_{I,2}], \quad (42a)$$

$$[R_{II,3}] = [R_{I,3}]. \quad (42b)$$

See Fig. 4 for the two-qubit tetrahedron of R_I and R_{II} .

It is expected that the Yang-Baxter gate R_{III} is locally equivalent to R_I and R_{II} , since B_I , B_{II} , and B_{III} have similar geometric representations (all on the edge A_2A_3 of the two-qubit tetrahedron). Through some calculations, we find

$$[R_{III,1}] = [a_{III,1}, a_{III,1}, c_{III,1}], \quad (43)$$

with

$$a_{III,1} = \arccos \left(\frac{\sqrt{1 - \cos 4\varphi_1}}{\cosh 4\mu - \cos 4\varphi_1} \right), \quad (44a)$$

$$c_{III,1} = \frac{i}{2} \ln \left(\frac{\sin(2\varphi_1 + 2i\mu)}{\sin(2\varphi_1 - 2i\mu)} \right). \quad (44b)$$

Compare with the nonlocal parameters of $R_{I,1}$ in Eq. (37), then we find that $R_{I,1}$ and $R_{III,1}$ have the correspondence through $2\varphi_1 \leftrightarrow \varphi$ and $2\mu \leftrightarrow \mu$. Therefore, $R_{III,1}$ is also on the faces OA_1A_2 and OA_2A_3 of the two-qubit tetrahedron. See Fig. 4.

The second and third kinds of R_{III} have the nonlocal parameters

$$[R_{III,2}] = \left[\frac{\pi}{2}, \frac{\pi}{2}, \frac{\pi}{2} - 2\varphi_{III,2} \right], \quad (45a)$$

$$[R_{III,3}] = \left[\frac{\pi}{2}, \frac{\pi}{2}, \frac{\pi}{2} - 2\varphi_{III,3} \right], \quad (45b)$$

with

$$\varphi_{III,2} = \arccos \left(\frac{\sinh \mu \cos \varphi_1}{\sqrt{\sinh^2 \mu \cos^2 \varphi_1 + \cosh^2 \mu \sin^2 \varphi_1}} \right), \quad (46a)$$

$$\varphi_{III,3} = \arccos \left(\frac{\cosh \mu \cos \varphi_1}{\sqrt{\cosh^2 \mu \cos^2 \varphi_1 + \sinh^2 \mu \sin^2 \varphi_1}} \right). \quad (46b)$$

Therefore, $R_{III,2}$ and $R_{III,3}$ are on the edge A_2A_3 of the two-qubit tetrahedron. See Fig. 4. When $\mu = 0$, $R_{III,2}$ becomes locally equivalent to the SWAP gate. While $R_{III,3}$ requires $\varphi_1 = \pi/2$ to be locally equivalent to the SWAP gate.

The Yang-Baxter gate R_{IV} generated from B_{IV} has the nonlocal parameters

$$[R_{IV}] = [2\chi, 0, 0], \quad (47)$$

with the spectral parameter χ defined in Eq. (36). It represents the edge OA_1 of the two-qubit tetrahedron. See Fig. 4. From Eq. (35), we can easily see that $R_{IV}(\chi = 0) \cong \mathbb{1}_4$ and $R_{IV}(\chi = \pi/2)$ is locally equivalent to $\sigma_x \otimes \sigma_x$.

D. Gate decompositions of Yang-Baxter gates

Based on the nonlocal parameters of the Yang-Baxter gates, we find the optimal gate decomposition (with the minimal number of CNOTs) of R_I and R_{III} in terms of the universal gate set $\{R_z(\theta), H, \text{CNOT}\}$. See Figs. 5 and 6. For R_I , we define the parameter ω as

$$\omega = \frac{1}{2}(\varphi_2 - \varphi_3), \quad (48)$$

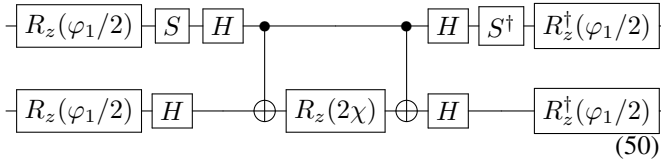
which only appears in the single-qubit gates of the decomposition. It is also called the q deformation parameter of the R matrix [77].

Note that R_I and R_{II} have the relation

$$R_{I,1,2,3} = (\mathbb{1}_2 \otimes \sigma_x) R_{II,1,2,3} (\mathbb{1}_2 \otimes \sigma_x), \quad (49)$$

suggested by Eq. (29), therefore the gate decompositions of R_{II} are almost identical with R_I . When $R_{l,2,3}$ with $l \in \{I, II, III\}$ are at A_2 of the two-qubit tetrahedron, their decompositions only require two CNOTs. Similarly, when $R_{l,1}$ with $l \in \{I, II, III\}$ are at the edge OA_2 or A_1A_2 (with one vanishing nonlocal parameter), only two CNOTs are required.

Notice that the Yang-Baxter gate R_{IV} has two vanishing nonlocal parameters, therefore at most two CNOTs are needed for its construction. The optimal decomposition of R_{IV} is



with the braid gate parameter φ_1 and the spectral parameter χ . The gate identity (11) has been applied.

Based on the gate decomposition of R_I shown in Fig. 5, the necessary and sufficient condition for R_I to be the Clifford gate is $\omega \in \{k\pi, k \in \mathbb{Z}\}$, and $a_{I,1}, c_{I,1}, \varphi_{I,2}, \varphi_{I,3} \in \{k\pi/2, k \in \mathbb{Z}\}$. Specifically, the $R_{I,1}$ is a Clifford gate if $\mu = 0$, or $\varphi \in \{k\pi, k \in \mathbb{Z}\}$. The former case gives the trivial identity gate, while the latter is locally equivalent to the SWAP gate. For $R_{I,2}$ and $R_{I,3}$, when $\mu = 0$ or $\varphi \in \{k\pi, k \in \mathbb{Z}\}$, we have $\varphi_{I,2}$ equal to 0 or π , which gives the locally equivalent SWAP gate (therefore to be the Clifford gate). Additionally, if the spectral parameter μ satisfies

$$\tanh\left(\frac{\mu}{2}\right) = \pm \tan\left(\frac{\varphi}{2}\right), \quad (51)$$

we can also have $R_{I,2}$ as the Clifford gate, which is locally equivalent to the iSWAP gate. For $R_{I,3}$, it is also true if

$$\tanh\left(\frac{\mu}{2}\right) = \pm \cot\left(\frac{\varphi}{2}\right), \quad (52)$$

is satisfied, which is the correspondence $\varphi \rightarrow \pi/2 - \varphi$ from Eq. (51).

The analysis on R_{II} to be the Clifford gate is the same as R_I due to the relation (49). For the case R_{III} , we see that there are T gates in the decompositions. See Fig. 6. Therefore, the necessary and sufficient condition for R_{III} to be the Clifford gate becomes $\varphi_2 \in \{k\pi + \pi/2, k \in \mathbb{Z}\}$, and $a_{III,1}, c_{III,1}, \varphi_{III,2}, \varphi_{III,3} \in \{k\pi/2, k \in \mathbb{Z}\}$. Specifically, the condition $a_{III,1}, c_{III,1} \in \{k\pi/2, k \in \mathbb{Z}\}$ (for $R_{III,1}$ to be the Clifford gate) is satisfied if $\mu = 0$ or $\varphi_1 \in \{k\pi/2, k \in \mathbb{Z}\}$. It is similar with $R_{I,1}$. When $\mu = 0$ or $\varphi_1 \in \{k\pi + \pi/2, k \in \mathbb{Z}\}$, we have the Clifford $R_{III,2}$, which is locally equivalent to iSWAP gate; when $\varphi_1 \in \{k\pi, k \in \mathbb{Z}\}$, we have the Clifford $R_{III,2}$, which is locally equivalent to SWAP gate. Similar results are applied to $R_{III,3}$. The Yang-Baxter gate R_{IV} is Clifford gate if $\varphi_1 \in \{k\pi, k \in \mathbb{Z}\}$ and $\chi \in \{k\pi/4, k \in \mathbb{Z}\}$, which is locally equivalent to CNOT. We summary the results in Table II.

The matchgate must have a vanishing nonlocal parameter [70]. We find that the $R_{I,1}$ gate is a nontrivial matchgate (not proportional to the identity operator) if $\varphi = \pi/2$. The $R_{I,2}$ gate is a matchgate if it is locally equivalent to the iSWAP gate where the spectral parameter satisfies the Eq. (51). The $R_{I,3}$ gate has the similar results. Note that the Pauli transformation (49) preserves the matchgate. Therefore R_{II} is the matchgate if R_I is the matchgate with the same parameters. In the case of R_{III} , it can not be a nontrivial matchgate, similar to B_{III} . While R_{IV} is always a matchgate independent of the spectral parameter.

The dual unitary two-qubit gates are on the edge A_2A_3 of the two-qubit tetrahedron [50]. Therefore, $R_{l,2}$ and $R_{l,3}$ with $l \in \{I, II, III\}$ are always dual unitary independent on the spectral parameter. However, R_{IV} can not be the dual unitary gate, since it is on the edge OA_1 . See Fig. 4. When $R_{l,1}$ with $l \in \{I, II, III\}$ reduces to the corresponding braid gate (by taking the spectral parameter $x = 0$), it is on the edge A_2A_3 , therefore are dual unitary.

E. Entangling powers

The entangling power of the two-qubit gate defined in Eq. (9) quantifies the ability to generate entanglement from the product state. It can be viewed as the interacting strength between qubits in the brick-wall circuits [51]. Given the nonlocal parameters of R_I , we numerically calculate its entangling powers in terms of the braid gate parameter φ and the spectral parameter μ . See Fig. 7. When $\mu = 0$ or $\varphi \in \{k\pi, k \in \mathbb{Z}\}$, $R_{I,1,2,3}$ has the zero entangling power, corresponding to the trivial two-qubit gate or SWAP gate. When $\mu \rightarrow \infty$ and $\varphi \in \{k\pi + \pi/2, k \in \mathbb{Z}\}$, $R_{I,1,2,3}$ has the maximal entangling power, corresponding to the iSWAP gate. Note that $\mu \leftrightarrow -\mu$ does not change the magnitude of the nonlocal parameters and the entangling power, therefore we only draw $\mu \geq 0$ in Fig. 7.

The entangling powers of $R_{II,1,2,3}$ are exactly same as $R_{I,1,2,3}$ due to the relation of Eq. (49). The entangling powers of $R_{III,1}$ is qualitatively same as $R_{I,1}$ with the correspondence $2\varphi_1 \leftrightarrow \varphi$ and $2\mu \leftrightarrow \mu$. The Yang-Baxter gate R_{IV} has

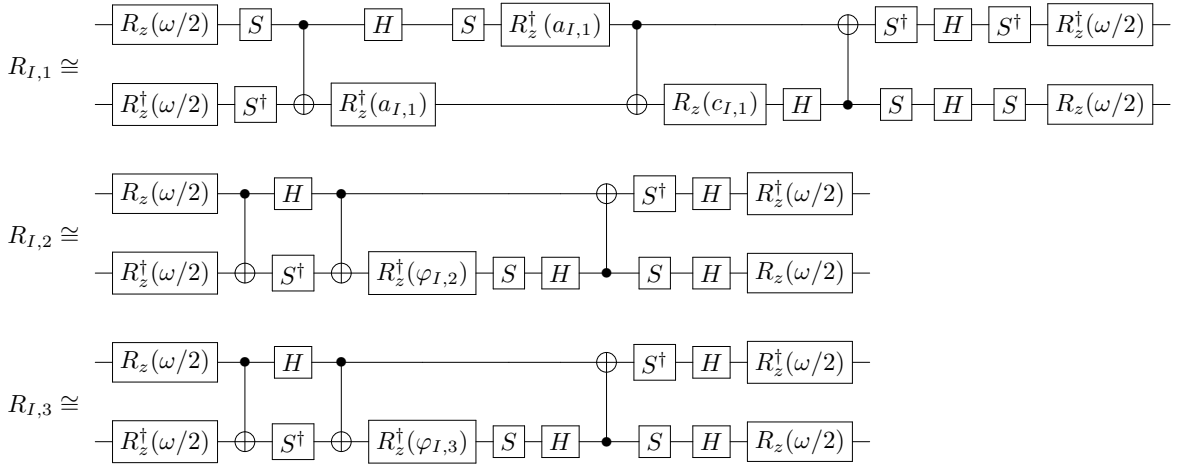


FIG. 5. Decomposition of Yang-Baxter gates $R_{I,1}$ (32), $R_{I,2}$ (34a), and $R_{I,3}$ (34b) into the universal gate set $\{R_z(\theta), H, \text{CNOT}\}$. The parameters $a_{I,1}$, $c_{I,1}$, $\varphi_{I,2}$, and $\varphi_{I,3}$ are nonlocal parameters given in Eqs. (38a), (38b), (41a), and (41b) respectively. The parameter ω is given in Eq. (48).

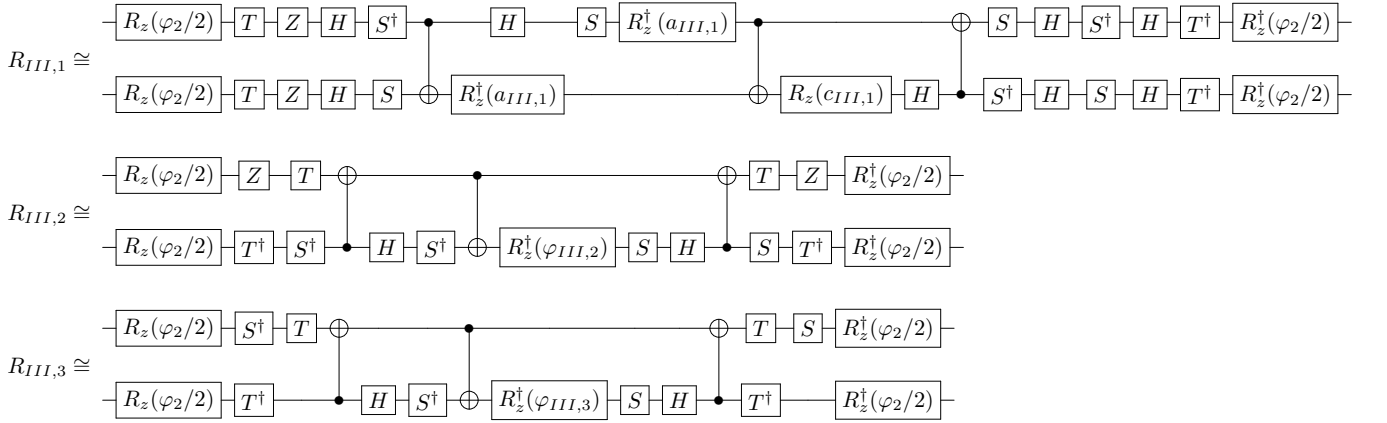


FIG. 6. Decomposition of Yang-Baxter gates $R_{III,1}$ (32), $R_{III,2}$ (34a), and $R_{III,3}$ (34b) into the universal gate set $\{R_z(\theta), H, \text{CNOT}\}$. The parameters $a_{III,1}$, $c_{III,1}$, $\varphi_{III,2}$, and $\varphi_{III,3}$ are nonlocal parameters given in Eqs. (44a), (44b), (46a), and (46b) respectively.

the entangling power

$$e_p(R_{IV}) = \frac{2}{9} \sin^2(2\chi), \quad (53)$$

which has the maximal at $\chi = \pi/4$, corresponding to B_{IV} . Note that the Yang-Baxter gates have the maximal entangling power corresponding to the point A_2 with the nonlocal parameters $[\pi/2, \pi/2, 0]$ (iSWAP gate), or the middle of OA_1 with the nonlocal parameters $[\pi/2, 0, 0]$ (CNOT gate).

V. CONCLUSIONS

In this work, we have studied the geometric representations of braid and Yang-Baxter gates, where the Yang-Baxter gates are obtained from the Yang-Baxterization of braid gates. Braid and Yang-Baxter gates on the same point of the two-qubit tetrahedron can be transformed from each other through

single-qubit gates. In the two-qubit tetrahedron representation, we find that the Yang-Baxter gates can only exist on the edges A_2A_3 and OA_1 , and on the faces OA_2A_3 and $A_1A_2A_3$. Based on their geometric representations, we give their gate decomposition in terms of the universal gate set $\{R_z(\theta), H, \text{CNOT}\}$ with the minimal number of CNOTs. We identify the parameters that make the braid and Yang-Baxter gates to be the Clifford gate, the matchgate, and the dual unitary gate. The braid and Yang-Baxter gates have the maximal entangling power if they are locally equivalent to iSWAP or CNOT.

Certainly, we do not cover all the Yang-Baxter gates in our study. Finding all (parameter dependent) solutions of the Yang-Baxter equation, even for the two-qubit representation, is challenging [80]. It would be interesting to check whether other Yang-Baxter gates can exist in other regions of the two-qubit tetrahedron. Our study can also be generalized to the unitary solution of the colored Yang-Baxter equation,

| | Clifford gate | Matchgate | Dual unitary gate |
|-------------|---|-----------------------|---------------------------|
| $R_{I,1}$ | $\omega \in \{k\pi, k \in \mathbb{Z}\}$ $\mu = 0$ or $\varphi \in \{k\pi, k \in \mathbb{Z}\}$ | $\varphi = \pi/2$ | $\mu \rightarrow -\infty$ |
| $R_{I,2}$ | $\omega \in \{k\pi, k \in \mathbb{Z}\}$ $\mu = 0$ or $\varphi \in \{k\pi, k \in \mathbb{Z}\}$ or Eq. (51) is satisfied | Eq. (51) is satisfied | Always |
| $R_{I,3}$ | $\omega \in \{k\pi, k \in \mathbb{Z}\}$ $\mu = 0$ or $\varphi \in \{k\pi, k \in \mathbb{Z}\}$ or Eq. (52) is satisfied | Eq. (52) is satisfied | Always |
| $R_{III,1}$ | $\varphi_2 \in \{k\pi + \pi/2, k \in \mathbb{Z}\}$ $\mu = 0$ or $\varphi_1 \in \{k\pi/2, k \in \mathbb{Z}\}$ | Cannot | $\mu \rightarrow -\infty$ |
| $R_{III,2}$ | $\varphi_2 \in \{k\pi + \pi/2, k \in \mathbb{Z}\}$ $\mu = 0$ or $\varphi_1 \in \{k\pi + \pi/2, k \in \mathbb{Z}\}$ or $\varphi_1 \in \{k\pi, k \in \mathbb{Z}\}$ | Cannot | Always |
| $R_{III,3}$ | $\varphi_2 \in \{k\pi + \pi/2, k \in \mathbb{Z}\}$ $\mu = 0$ or $\varphi_1 \in \{k\pi + \pi/2, k \in \mathbb{Z}\}$ or $\varphi_1 \in \{k\pi, k \in \mathbb{Z}\}$ | Cannot | Always |
| R_{IV} | $\varphi_1 \in \{k\pi, k \in \mathbb{Z}\}$ and $\chi \in \{k\pi/4, k \in \mathbb{Z}\}$ | Always | Cannot |

TABLE II. Conditions for Yang-Baxter gates defined in Eqs. (32), (34a), and (34b) to be the Clifford gate, the matchgate, and the dual unitary gate. The conditions for $R_{III,1,2,3}$ are the same as the conditions for $R_{II,1,2,3}$, therefore omitted in the table.

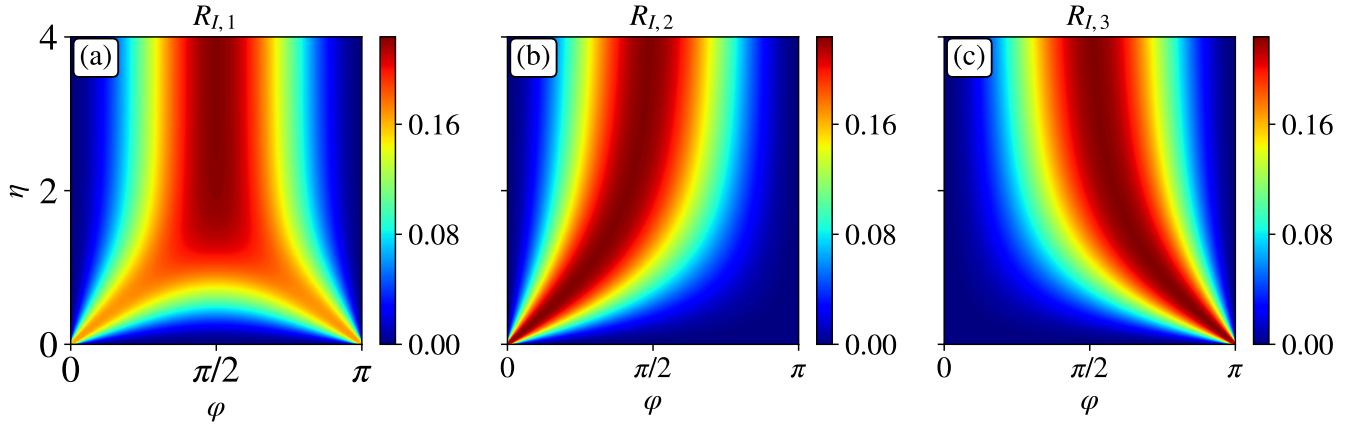


FIG. 7. Entangling powers of Yang-Baxter gates R_I obtained from braid gate B_I . Yang-Baxter gates $R_{I,1}$, $R_{I,2}$, and $R_{I,3}$ are defined in Eqs. (32), (34a), and (34b) respectively. Here $\mu = \ln(x)$ is the spectral parameter, and $\varphi = (\varphi_2 + \varphi_3)/2 - \varphi_1$ is the braid gate parameter.

also called the multi-parametric Yang–Baxter equation or the Yang-Baxter equation with non-additive spectral parameters [81, 82]. Most studies on the integrable circuit are limited to the one-dimensional qubit array. It is natural to study the unitary solutions of the tetrahedron equation, which is the multi-dimensional generalization of the Yang-Baxter equation [83–85]. In other words, the integrable circuits might be able to be generalized to the two-dimensional qubit array. We leave it for our future study.

ACKNOWLEDGMENTS

The work of K.Z. was supported by the National Natural Science Foundation of China under Grant Nos. 12305028 and

12247103, and the Youth Innovation Team of Shaanxi Universities. The work of K.H. was supported by the National Natural Science Foundation of China (Grant Nos. 12275214, 12247103, and 12047502), the Natural Science Basic Research Program of Shaanxi Province Grant Nos. 2021JCW-19 and 2019JQ-107, and Shaanxi Key Laboratory for Theoretical Physics Frontiers in China. K.Y. and V.K. are funded by the U.S. Department of Energy, Office of Science, National Quantum Information Science Research Centers, Co-Design Center for Quantum Advantage under Contract No. DE-SC0012704.

Appendix A: Proof of Theorem 2

Proof. Through Yang-Baxterization of the braid matrix with two distinct eigenvalues, we have

$$\begin{aligned} R(x) &= \left(x + \frac{\lambda_1}{\lambda_2}\right) P_1 + \left(1 + x \frac{\lambda_1}{\lambda_2}\right) P_2 \\ &= \frac{1}{\lambda_2} (B + x \lambda_1 \lambda_2 B^{-1}). \end{aligned} \quad (\text{A1})$$

Since we assume that B is unitary, therefore $|\lambda_1| = |\lambda_2| = 1$ and $B^{-1} = B^\dagger$. The unitary condition is given by

$$R(x)R^\dagger(x) = \mathbb{1} + |x|^2 + x \lambda_1 \lambda_2 B^{\dagger 2} + x^* \lambda_1^* \lambda_2^* B^2, \quad (\text{A2})$$

with the complex conjugate $*$. Through the spectral decomposition of B , we have

$$B^{\dagger 2} = \lambda_1^{*2} P_1 + \lambda_2^{*2} P_2 = \lambda_1^{*2} + \lambda_2^{*2} - \lambda_1^{*2} \lambda_2^{*2} B^2, \quad (\text{A3})$$

which gives

$$R(x)R^\dagger(x) = \mathbb{1} + |x|^2 + x (\lambda_1^* \lambda_2 + \lambda_2^* \lambda_1) + (x^* - x) \lambda_1^* \lambda_2^* B^2. \quad (\text{A4})$$

If $B^2 \neq \mathbb{1}$, the spectral parameter must be a real number for unitary $R(x)$. \square

Appendix B: matrix expression of Yang-Baxter gates

Consider the Yang-Baxter equations with the additive spectral parameter

$$\mu = \ln x, \quad (\text{B1})$$

and $x > 0$. The braid gates B_I and B_{II} give the Yang-Baxter gates

$$R_{I,1}(\mu) \cong \begin{pmatrix} 1 & 0 & 0 & 0 \\ 0 & \frac{\sin \varphi}{\sin(\varphi - i\mu)} & \frac{-ie^{i\omega} \sinh \mu}{\sin(\varphi - i\mu)} & 0 \\ 0 & \frac{-ie^{-i\omega} \sinh \mu}{\sin(\varphi - i\mu)} & \frac{\sin \varphi}{\sin(\varphi - i\mu)} & 0 \\ 0 & 0 & 0 & 1 \end{pmatrix}, \quad R_{II,1}(\mu) \cong \begin{pmatrix} \frac{\sin \varphi}{\sin(\varphi - i\mu)} & 0 & 0 & \frac{-ie^{i\omega} \sinh \mu}{\sin(\varphi - i\mu)} \\ 0 & 1 & 0 & 0 \\ 0 & 0 & 1 & 0 \\ \frac{-ie^{-i\omega} \sinh \mu}{\sin(\varphi - i\mu)} & 0 & 0 & \frac{\sin \varphi}{\sin(\varphi - i\mu)} \end{pmatrix}, \quad (\text{B2a})$$

$$R_{I,2}(\mu) \cong \frac{1}{\sqrt{\Delta_{I,2}}} \begin{pmatrix} \sinh\left(\frac{1}{2}(\mu + i\varphi)\right) & 0 & 0 & 0 \\ 0 & 0 & e^{i\omega} \sinh\left(\frac{1}{2}(\mu - i\varphi)\right) & 0 \\ 0 & e^{-i\omega} \sinh\left(\frac{1}{2}(\mu - i\varphi)\right) & 0 & 0 \\ 0 & 0 & 0 & \sinh\left(\frac{1}{2}(\mu + i\varphi)\right) \end{pmatrix}, \quad (\text{B2b})$$

$$R_{I,3}(\mu) \cong \frac{1}{\sqrt{\Delta_{I,3}}} \begin{pmatrix} \cosh\left(\frac{1}{2}(\mu + i\varphi)\right) & 0 & 0 & 0 \\ 0 & 0 & e^{i\omega} \cosh\left(\frac{1}{2}(\mu - i\varphi)\right) & 0 \\ 0 & e^{-i\omega} \cosh\left(\frac{1}{2}(\mu - i\varphi)\right) & 0 & 0 \\ 0 & 0 & 0 & \cosh\left(\frac{1}{2}(\mu + i\varphi)\right) \end{pmatrix}, \quad (\text{B2c})$$

$$R_{II,2}(\mu) \cong \frac{1}{\sqrt{\Delta_{II,2}}} \begin{pmatrix} 0 & 0 & 0 & e^{i\omega} \sinh\left(\frac{1}{2}(\mu - i\varphi)\right) \\ 0 & \sinh\left(\frac{1}{2}(\mu + i\varphi)\right) & 0 & 0 \\ 0 & 0 & \sinh\left(\frac{1}{2}(\mu + i\varphi)\right) & 0 \\ e^{-i\omega} \sinh\left(\frac{1}{2}(\mu - i\varphi)\right) & 0 & 0 & 0 \end{pmatrix}, \quad (\text{B2d})$$

$$R_{II,3}(\mu) \cong \frac{1}{\sqrt{\Delta_{II,3}}} \begin{pmatrix} 0 & 0 & 0 & e^{i\omega} \cosh\left(\frac{1}{2}(\mu - i\varphi)\right) \\ 0 & \cosh\left(\frac{1}{2}(\mu + i\varphi)\right) & 0 & 0 \\ 0 & 0 & \cosh\left(\frac{1}{2}(\mu + i\varphi)\right) & 0 \\ e^{-i\omega} \cosh\left(\frac{1}{2}(\mu - i\varphi)\right) & 0 & 0 & 0 \end{pmatrix}, \quad (\text{B2e})$$

with the defined parameters

$$\varphi = \frac{1}{2}(\varphi_2 + \varphi_3) - \varphi_1, \quad (\text{B3a})$$

$$\omega = \frac{1}{2}(\varphi_2 - \varphi_3), \quad (\text{B3b})$$

and the normalizations

$$\Delta_{I,2} = \Delta_{II,2} = \sin^2\left(\frac{\phi}{2}\right) + \sinh^2\left(\frac{\mu}{2}\right), \quad (\text{B4a})$$

$$\Delta_{I,3} = \Delta_{II,3} = \cos^2\left(\frac{\phi}{2}\right) + \sinh^2\left(\frac{\mu}{2}\right). \quad (\text{B4b})$$

The three kinds of Yang-Baxter gates obtained from B_{III}

have the matrix expression

$$R_{III,1}(\mu) \cong \begin{pmatrix} \frac{\cosh \mu \cos \varphi_1}{\cosh(\mu + i\varphi_1)} & 0 & 0 & -e^{i\varphi_2} \frac{\sinh \mu \sin \varphi_1}{\cosh(\mu + i\varphi_1)} \\ 0 & i \frac{\cosh \mu \sin \varphi_1}{\sinh(\mu + i\varphi_1)} & -\frac{\sinh \mu \cos \varphi_1}{\sinh(\mu + i\varphi_1)} & 0 \\ 0 & -\frac{\sinh \mu \cos \varphi_1}{\sinh(\mu + i\varphi_1)} & i \frac{\cosh \mu \sin \varphi_1}{\sinh(\mu + i\varphi_1)} & 0 \\ e^{-i\varphi_2} \frac{\sinh \mu \sin \varphi_1}{\cosh(\mu + i\varphi_1)} & 0 & 0 & \frac{\cosh \mu \cos \varphi_1}{\cosh(\mu + i\varphi_1)} \end{pmatrix}, \quad (\text{B5a})$$

$$R_{III,2}(\mu) \cong \frac{1}{\sqrt{\Delta_{III,2}}} \begin{pmatrix} \sinh \mu \cos \varphi_1 & 0 & 0 & e^{i\varphi_2} \cosh \mu \sin \varphi_1 \\ 0 & i \cosh \mu \sin \varphi_1 & -\sinh \mu \cos \varphi_1 & 0 \\ 0 & -\sinh \mu \cos \varphi_1 & i \cosh \mu \sin \varphi_1 & 0 \\ -e^{-i\varphi_2} \cosh \mu \sin \varphi_1 & 0 & 0 & \sinh \mu \cos \varphi_1 \end{pmatrix}, \quad (\text{B5b})$$

$$R_{III,3}(\mu) \cong \frac{1}{\sqrt{\Delta_{III,3}}} \begin{pmatrix} \cosh \mu \cos \varphi_1 & 0 & 0 & -e^{i\varphi_2} \sinh \mu \sin \varphi_1 \\ 0 & i \sinh \mu \sin \varphi_1 & -\cosh \mu \cos \varphi_1 & 0 \\ 0 & -\cosh \mu \cos \varphi_1 & i \sinh \mu \sin \varphi_1 & 0 \\ e^{-i\varphi_2} \sinh \mu \sin \varphi_1 & 0 & 0 & \cosh \mu \cos \varphi_1 \end{pmatrix}, \quad (\text{B5c})$$

with the normalizations

$$\Delta_{III,2} = \sinh^2 \mu \cos^2 \varphi_1 + \cosh^2 \mu \sin^2 \varphi_1, \quad (\text{B6a})$$

$$\Delta_{III,3} = \cosh^2 \mu \cos^2 \varphi_1 + \sinh^2 \mu \sin^2 \varphi_1. \quad (\text{B6b})$$

-
- [1] M. A. Nielsen and I. L. Chuang, *Quantum Computation and Quantum Information: 10th Anniversary Edition* (2010).
- [2] J. Preskill, Quantum computing in the nisq era and beyond, *Quantum* **2**, 79 (2018).
- [3] D. P. DiVincenzo, Two-bit gates are universal for quantum computation, *Physical Review A* **51**, 1015 (1995).
- [4] A. Barenco, C. H. Bennett, R. Cleve, D. P. DiVincenzo, N. Margolus, P. Shor, T. Sleator, J. A. Smolin, and H. Weinfurter, Elementary gates for quantum computation, *Physical Review A* **52**, 3457 (1995).
- [5] B. Sutherland, *Beautiful models: 70 years of exactly solved quantum many-body problems* (World Scientific, 2004).
- [6] R. J. Baxter, *Exactly solved models in statistical mechanics* (Elsevier, 2016).
- [7] C.-N. Yang, Some exact results for the many-body problem in one dimension with repulsive delta-function interaction, *Physical Review Letters* **19**, 1312 (1967).
- [8] C. N. Yang, S matrix for the one-dimensional n-body problem with repulsive or attractive δ -function interaction, *Physical Review* **168**, 1920 (1968).
- [9] R. J. Baxter, Partition function of the eight-vertex lattice model, *Annals of Physics* **70**, 193 (1972).
- [10] L. Takhtadzhian and L. D. Faddeev, The quantum method of the inverse problem and the heisenberg xyz model, *Russian Mathematical Surveys* **34**, 11 (1979).
- [11] V. E. Korepin, N. M. Bogoliubov, and A. G. Izergin, *Quantum inverse scattering method and correlation functions*, Vol. 3 (Cambridge university press, 1997).
- [12] M. T. Batchelor and A. Foerster, Yang–baxter integrable models in experiments: from condensed matter to ultracold atoms, *Journal of Physics A: Mathematical and Theoretical* **49**, 173001 (2016).
- [13] H. Dye, Unitary solutions to the yang–baxter equation in dimension four, *Quantum Information Processing* **2**, 117 (2003).
- [14] L. H. Kauffman, *Knots and physics*, Vol. 1 (World scientific, 2001).
- [15] L. H. Kauffman and S. J. Lomonaco, Quantum entanglement and topological entanglement, *New Journal of Physics* **4**, 73 (2002).
- [16] L. H. Kauffman and S. J. Lomonaco, Braiding operators are universal quantum gates, *New Journal of Physics* **6**, 134 (2004).
- [17] G. Alagic, M. Jarret, and S. P. Jordan, Yang–baxter operators need quantum entanglement to distinguish knots, *Journal of Physics A: Mathematical and Theoretical* **49**, 075203 (2016).
- [18] L. H. Kauffman and E. Mehrotra, Topological aspects of quantum entanglement, *Quantum Information Processing* **18**, 1

- (2019).
- [19] G. M. Quinta and R. André, Classifying quantum entanglement through topological links, *Physical Review A* **97**, 042307 (2018).
- [20] P. Padmanabhan, F. Sugino, and D. Trancanelli, Local invariants of braiding quantum gates—associated link polynomials and entangling power, *Journal of Physics A: Mathematical and Theoretical* **54**, 135301 (2021).
- [21] Y. Zhang, Teleportation, braid group and Temperley–Lieb algebra, *Journal of Physics A: Mathematical and General* **39**, 11599 (2006).
- [22] J.-L. Chen, K. Xue, and M.-L. Ge, Braiding transformation, entanglement swapping, and Berry phase in entanglement space, *Physical Review A* **76**, 042324 (2007).
- [23] Y. Zhang, K. Zhang, and J. Pang, Teleportation-based quantum computation, extended Temperley–Lieb diagrammatical approach and Yang–Baxter equation, *Quantum Information Processing* **15**, 405 (2016).
- [24] K. Zhang and Y. Zhang, Quantum teleportation and Birman–Murakami–Wenzl algebra, *Quantum Information Processing* **16**, 1 (2017).
- [25] M. Vanicat, L. Zadnik, and T. Prosen, Integrable Trotterization: local conservation laws and boundary driving, *Physical Review Letters* **121**, 030606 (2018).
- [26] M. Ljubotina, L. Zadnik, and T. Prosen, Ballistic spin transport in a periodically driven integrable quantum system, *Physical Review Letters* **122**, 150605 (2019).
- [27] A. J. Friedman, S. Gopalakrishnan, and R. Vasseur, Integrable many-body quantum Floquet– Thouless pumps, *Physical Review Letters* **123**, 170603 (2019).
- [28] Y. Miao, V. Gritsev, and D. V. Kurlov, The Floquet Baxterization, *SciPost Physics* **16**, 078 (2024).
- [29] I. L. Aleiner, Bethe ansatz solutions for certain periodic quantum circuits, *Annals of Physics* **433**, 168593 (2021).
- [30] P. W. Claeys, J. Herzog-Arbeitman, and A. Lamacraft, Correlations and commuting transfer matrices in integrable unitary circuits, *SciPost Physics* **12**, 007 (2022).
- [31] K. Maruyoshi, T. Okuda, J. W. Pedersen, R. Suzuki, M. Yamazaki, and Y. Yoshida, Conserved charges in the quantum simulation of integrable spin chains, *Journal of Physics A: Mathematical and Theoretical* **56**, 165301 (2023).
- [32] E. Vernier, H.-C. Yeh, L. Piroli, and A. Mitra, Strong zero modes in integrable quantum circuits, arXiv preprint arXiv:2401.12305 [10.48550/arXiv.2401.12305](https://arxiv.org/abs/2401.12305) (2024).
- [33] A. Hutsalyuk, Y. Jiang, B. Pozsgay, H. Xu, and Y. Zhang, Exact spin correlators of integrable quantum circuits from algebraic geometry, arXiv preprint arXiv:2405.16070 [10.48550/arXiv.2005.06468](https://arxiv.org/abs/2405.16070) (2024).
- [34] L. Zadnik, M. Ljubotina, Ž. Krajnik, E. Ilievski, and T. Prosen, Quantum many-body spin ratchets, arXiv preprint arXiv:2406.01571 [10.48550/arXiv.2406.01571](https://arxiv.org/abs/2406.01571) (2024).
- [35] Y. Zhang, Quantum computing via the Bethe ansatz, *Quantum Information Processing* **11**, 585 (2012).
- [36] Y. Zhang, Integrable quantum computation, *Quantum Information Processing* **12**, 631 (2013).
- [37] L. Banchi, E. Compagno, V. Korepin, and S. Bose, Quantum gates between distant qubits via spin-independent scattering, *Quantum* **1**, 36 (2017).
- [38] A. Morvan, T. I. Andersen, X. Mi, C. Neill, A. Petukhov, K. Kechedzhi, D. Abanin, A. Michailidis, R. Acharya, F. Arute, *et al.*, Formation of robust bound states of interacting microwave photons, *Nature* **612**, 240 (2022).
- [39] Y. Kim, A. Eddins, S. Anand, K. X. Wei, E. Van Den Berg, S. Rosenblatt, H. Nayfeh, Y. Wu, M. Zaletel, K. Temme, *et al.*, Evidence for the utility of quantum computing before fault tolerance, *Nature* **618**, 500 (2023).
- [40] N. Keenan, N. F. Robertson, T. Murphy, S. Zhuk, and J. Goold, Evidence of Kardar–Parisi–Zhang scaling on a digital quantum simulator, *npj Quantum Information* **9**, 72 (2023).
- [41] O. Shtanko, D. S. Wang, H. Zhang, N. Harle, A. Seif, R. Movassagh, and Z. Mineev, Uncovering local integrability in quantum many-body dynamics, arXiv preprint arXiv:2307.07552 [10.48550/arXiv.2307.07552](https://arxiv.org/abs/2307.07552) (2023).
- [42] J. Zhang, J. Vala, S. Sastry, and K. B. Whaley, Geometric theory of nonlocal two-qubit operations, *Physical Review A* **67**, 042313 (2003).
- [43] V. Jones, Baxterization, *International Journal of Modern Physics B* **04**, 701 (1990).
- [44] Y. Cheng, M. L. Ge, and K. Xue, Yang–Baxterization of braid group representations, *Communications in Mathematical Physics* **136**, 195 (1991).
- [45] M.-L. Ge, Y.-S. Wu, and K. Xue, Explicit trigonometric Yang–Baxterization, *International Journal of Modern Physics A* **06**, 3735 (1991).
- [46] D. Gottesman, Stabilizer Codes and Quantum Error Correction (1997), [quant-ph/9705052](https://arxiv.org/abs/quant-ph/9705052).
- [47] D. Gottesman, Theory of fault-tolerant quantum computation, *Physical Review A* **57**, 127 (1998).
- [48] L. G. Valiant, Quantum computers that can be simulated classically in polynomial time, in *Proceedings of the Thirty-Third Annual ACM Symposium on Theory of Computing*, STOC '01 (Association for Computing Machinery, New York, NY, USA, 2001) pp. 114–123.
- [49] R. Jozsa and A. Miyake, Matchgates and classical simulation of quantum circuits, *Proceedings of the Royal Society A: Mathematical, Physical and Engineering Sciences* **464**, 3089 (2008).
- [50] B. Bertini, P. Kos, and T. Prosen, Exact Correlation Functions for Dual-Unitary Lattice Models in $1+1$ Dimensions, *Physical Review Letters* **123**, 210601 (2019).
- [51] D. Hahn and L. Colmenarez, Absence of localization in weakly interacting Floquet circuits, *Physical Review B* **109**, 094207 (2024).
- [52] B. Kraus and J. I. Cirac, Optimal creation of entanglement using a two-qubit gate, *Physical Review A* **63**, 062309 (2001).
- [53] Y. Makhlin, Nonlocal properties of two-qubit gates and mixed states and optimization of quantum computations, *Quantum Information Processing* **1**, 243 (2002).
- [54] T. Tanamoto, Y.-x. Liu, X. Hu, and F. Nori, Efficient quantum circuits for one-way quantum computing, *Physical Review Letters* **102**, 100501 (2009).
- [55] P. Zanardi, C. Zalka, and L. Faoro, Entangling power of quantum evolutions, *Physical Review A* **62**, 030301 (2000).
- [56] S. Balakrishnan and R. Sankaranarayanan, Entangling power and local invariants of two-qubit gates, *Physical Review A* **82**, 034301 (2010).
- [57] J.-L. Brylinski and R. Brylinski, Universal quantum gates, in *Mathematics of Quantum Computation* (Chapman and Hall/CRC, 2002) pp. 117–134.
- [58] M. J. Bremner, C. M. Dawson, J. L. Dodd, A. Gilchrist, A. W. Harrow, D. Mortimer, M. A. Nielsen, and T. J. Osborne, Practical scheme for quantum computation with any two-qubit entangling gate, *Physical Review Letters* **89**, 247902 (2002).
- [59] J. Zhang, J. Vala, S. Sastry, and K. B. Whaley, Optimal quantum circuit synthesis from controlled-unitary gates, *Physical Review A* **69**, 042309 (2004).
- [60] G. Vidal and C. M. Dawson, Universal quantum circuit for two-qubit transformations with three controlled-NOT gates, *Physical Review A* **69**, 010301 (2004).

- [61] F. Vatan and C. Williams, Optimal quantum circuits for general two-qubit gates, *Physical Review A* **69**, 032315 (2004).
- [62] V. V. Shende, I. L. Markov, and S. S. Bullock, Minimal universal two-qubit controlled-NOT-based circuits, *Physical Review A* **69**, 062321 (2004).
- [63] Y.-S. Zhang, M.-Y. Ye, and G.-C. Guo, Conditions for optimal construction of two-qubit nonlocal gates, *Physical Review A* **71**, 062331 (2005).
- [64] K. Zhang, K. Yu, K. Hao, and V. Korepin, Optimal Realization of Yang–Baxter Gate on Quantum Computers, *Advanced Quantum Technologies* **7**, 2300345 (2024).
- [65] J. Hietarinta, All solutions to the constant quantum Yang-Baxter equation in two dimensions, *Physics Letters A* **165**, 245 (1992).
- [66] H. A. Dye, Unitary Solutions to the Yang–Baxter Equation in Dimension Four, *Quantum Information Processing* **2**, 117 (2003).
- [67] P. Padmanabhan, F. Sugino, and D. Trancanelli, Braiding quantum gates from partition algebras, *Quantum* **4**, 311 (2020).
- [68] P. Padmanabhan, F. Sugino, and D. Trancanelli, Local invariants of braiding quantum gates—associated link polynomials and entangling power, *Journal of Physics A: Mathematical and Theoretical* **54**, 135301 (2021).
- [69] B. M. Terhal and D. P. DiVincenzo, Classical simulation of noninteracting-fermion quantum circuits, *Physical Review A* **65**, 032325 (2002).
- [70] D. J. Brod and E. F. Galvão, Extending matchgates into universal quantum computation, *Physical Review A* **84**, 022310 (2011), 1106.1863 [quant-ph].
- [71] M. Jimbo, *Yang-Baxter equation in integrable systems*, Vol. 10 (World Scientific, 1990).
- [72] J. H. Perk and H. Au-Yang, Yang-Baxter equations, *Encyclopedia of Mathematical Physics* **5**, 465 (2006).
- [73] Y. Zhang, L. H. Kauffman, and M.-L. Ge, Universal quantum gate, yang–baxterization and hamiltonian, *International Journal of Quantum Information* **3**, 669 (2005).
- [74] Y. Zhang, L. H. Kauffman, and M.-L. Ge, Yang–baxterizations, universal quantum gates and hamiltonians, *Quantum Information Processing* **4**, 159 (2005).
- [75] J. S. Birman and H. Wenzl, Braids, link polynomials and a new algebra, *Transactions of the American Mathematical Society* **313**, 249 (1989).
- [76] J. Murakami, The Kauffman polynomial of links and representation theory, *Osaka Journal of Mathematics* **24**, 745 (1987).
- [77] A. Doikou, S. Evangelisti, G. Feverati, and N. Karaiskos, Introduction to quantum integrability, *International Journal of Modern Physics A* **25**, 3307 (2010).
- [78] D. Arnaudon, J. Avan, L. Frappat, E. Ragoucy, and M. Rossi, Towards a cladistics of double yangians and elliptic algebras, *Journal of Physics A: Mathematical and General* **33**, 6279 (2000).
- [79] W.-L. Yang and Y. Zhen, Modular transformation and twist between trigonometric limits of $sl(n)$ elliptic r-matrix, *Commun. Theor. Phys.(Beijing, China)* **36**, 131 (2001).
- [80] A. Garkun, S. K. Barik, A. K. Fedorov, V. Gritsev, *et al.*, New spectral-parameter dependent solutions of the yang-baxter equation, arXiv preprint arXiv:2401.12710 10.48550/arXiv.2401.12710 (2024).
- [81] Y.-Z. Zhang and J. L. Werry, New r-matrices with non-additive spectral parameters and integrable models of strongly correlated fermions, *Journal of High Energy Physics* **2020**, 1 (2020).
- [82] P. Padmanabhan, K. Hao, and V. Korepin, Integrability and non-invertible symmetries of projector spin chains, arXiv preprint arXiv:2401.05662 10.48550/arXiv.2401.05662 (2024).
- [83] A. Zamolodchikov, Tetrahedron equations and the relativistic s-matrix of straight-strings in $2+1$ -dimensions, *Communications in Mathematical Physics* **79**, 489 (1981).
- [84] P. Padmanabhan and V. Korepin, Solving the yang-baxter, tetrahedron and higher simplex equations using clifford algebras, arXiv preprint arXiv:2404.11501 <https://doi.org/10.48550/arXiv.2404.11501> (2024).
- [85] A. Sinha, P. Padmanabhan, and V. Korepin, Toffoli gates solve the tetrahedron equations, arXiv preprint arXiv:2405.16477 <https://doi.org/10.48550/arXiv.2405.16477> (2024).